3

Enthalpy, Entropy, and Volume Changes of Electron Transfer Reactions in Photosynthetic Proteins

Harvey J.M. Hou
University of Massachusetts Dartmouth
USA

1. Introduction

Photosynthesis involves a series of electron transfer steps to convert the sunlight energy into the chemical energy in green plants, algae, and cynobacteria. The three–dimensional structures of photosynthetic reaction centers at the high resolution uncover the binding sites and precise orientation of cofactors and their interaction with proteins and provided an excellent model to investigate the mechanism of electron transfer reaction. To understand fully an electron transfer reaction, it is necessary to understand not just its kinetics, but also thermodynamics. However, in contrast to the kinetics of electron transfer mechanisms, thermodynamic information is far less accessible. Thermodynamics reveals the energy levels of reactants and products, as well as the driving forces in the reaction. The driving force of the chemical reaction is the Gibbs free energy, which is composed of enthalpic and entropic components.

Pulsed photoacoustics provides direct measurements of enthalpy and volume changes of electron transfer. Using pulsed photoacoustics, the volume change and enthalpy of electron transfer reaction were measured in the photosynthetic reaction center complex of *Rb. sphaeroides*. A large entropy was calculated based on these measurements. Further photoacoustic measurements indicated that the entropy change of electron transfer in photosystem I from *Synechocystis* sp. PCC 6803 is similar to that in bacterial center. The deconvolution fit of the photoacoustic waves distinguished thermodynamic parameters of a large negative enthalpy change and large volume change for $P_{700}^* \rightarrow A_1$ step and a positive enthalpy change and a small volume change for $A_1^- \rightarrow F_{A/B}$ step. To explore the specific role of protein matrix, the *menA* and *menB* genes were inactivated by molecular genetics and showed the altered thermodynamics of electron transfer. Inactivating the *menG* gene causes 2–phytyl–1,4–naphthoquinone (Q) to be presented as a quinone acceptor. The fit by convolution of *menG* photoacoustic waves resolved a large volume contraction for the P700* $\rightarrow$ Q step and a positive volume change for the $Q^- \rightarrow F_{A/B}$ step. The photoacoustic data of the bacterial reaction center, *menA/B* mutant, *menG* mutant, and wild type phtosystem I show significant positive entropy. In contrast, electron transfer in photosystem II is accompanied by a small negative entropy change. *In vivo* photoacoustic measurements confirmed the difference in entropy between photosysmte I and photosystem II. We conclude that apparent entropy may play a vital role in photosynthetic electron transfers.

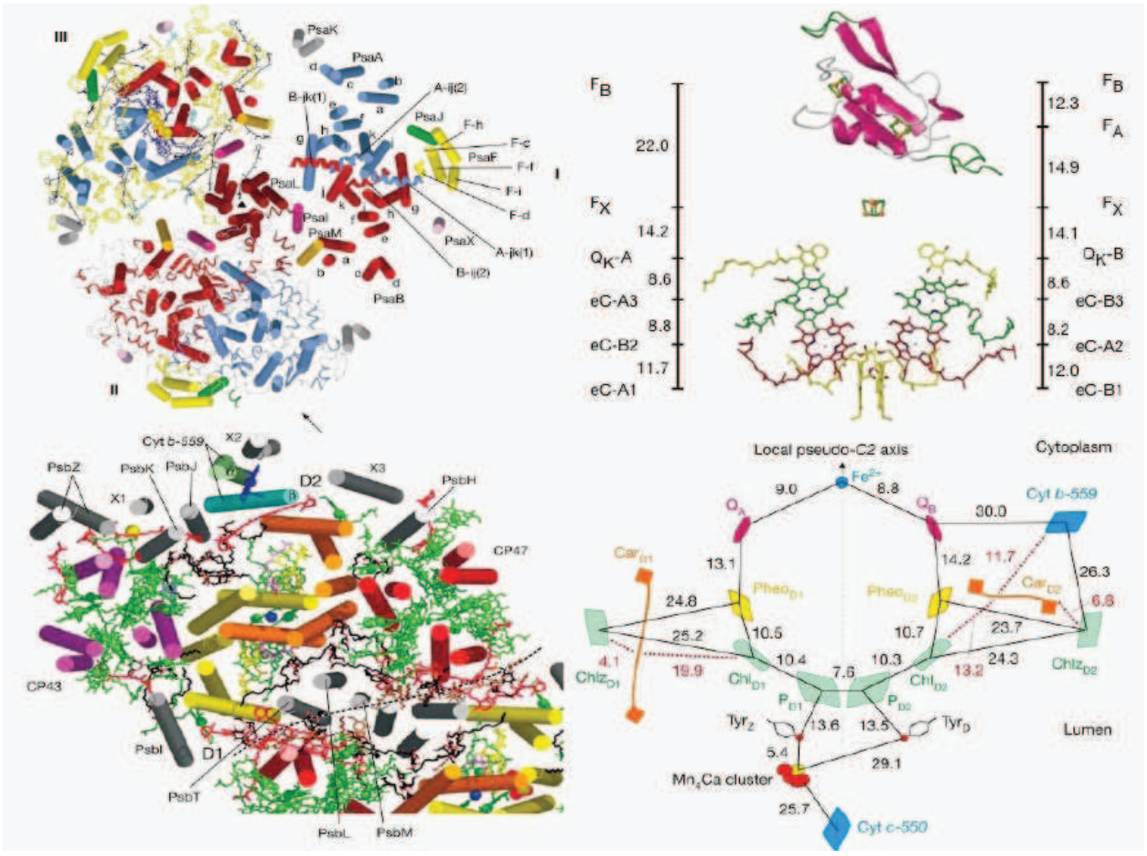

Fig. 1. Structures and arrangement of cofactors in PS I (upper) (Jordan et al., 2001) and PS II (lower) (reproduced with permission from Nature publishing Group (Loll et al., 2005)).

In this chapter we will present an overview of the protein structure and the electron transfer pathways of photosynthetic reaction centers and highlight the recent advances of thermodynamic aspects of these photosynthetic electron transfer reactions on the microsecond and nanosecond time scales using photoacoustics. The principle and experimental procedures of the pulsed photoacoustic methodology will be presented. The main focus of the chapter will be placed on the determinations, interpretations, and future endeavors of the thermodynamic parameters including the enthalpy, entropy, and volume changes of electron transfer reactions in the photosynthetic reaction centers of purple bacteria, cyanobacteria, and green plants *in vitro* and *in vivo*. The enthalpy, entropy, and volume changes of electron transfer in proteins provide novel insights into the role of the membrane environment and cofactors *in vitro* and *in vivo* in terms of a broadly thermodynamic view. These unique features offer the potential for a deeper understanding of the mechanisms of electron transfer in chemical and biological systems. They also present a framework to modify and improve the existing Marcus electron transfer theory as well as the formulation of a comprehensive electron transfer theory.

2. Protein structures, kinetics and thermodynamics in photosynthesis

Photosynthesis is the only process for large-scale solar energy storage in nature, in which the light photon energy is harvested by specific photosynthetic ligtht harvesting protein

complexes in thylakoid membranes and transfered to the reaction center. The key step of energy conversion occurs in the photosynthetic reaction centers. The three-dimensional structures of both Type I (Jordan et al., 2001; Amunts et al., 2007) and Type II (Ferreira et al., 2004; Loll et al., 2005) photosynthetic reaction centers have been determined at the atomic to molecular level. Figure 1 shows the structures and arrangement of cofactors of cyanobacterial photosystems I (PS I) at 2.5 Å resolution (Jordan et al., 2001) and of cyanobacterial PS II at 3.0 Å resolution (Loll et al., 2005). These structures reveal the binding sites and precise orientation of cofactors and their interaction with proteins and provide a solid basis to interpret results of photoacoustic studies at an atomic level.

On the basis of the high-resolution structural information, the kinetics and thermodynamics of electron transfer reactions in biological systems are required for understanding precise mechanisms. During the past decade the kinetics of electron transfer steps in reaction centers of anoxygenic and oxygenic photosynthesis has been thoroughly investigated over the timescale of femtosecond to second (Brettel, 1997; Dekker & Van Grondelle, 2000; Brettel and Leibl, 2001; Gobets & van Grondelle, 2001) as shown in Figure 2. These works revealed the electron pathway and identified almost the entire electron transfer intermediates in both photosystems. However, the thermodynamics of electron transfer steps in photosynthesis, such as volume change, enthalpy and entropy, is far less well understood. There are at least two reasons to measure these thermodynamic parameters accurately. First, knowledge of the thermodynamic parameters of electron transfer reactions allows one to gauge the efficiency of energy conversion, Efficiency refers to the amount of the solar energy stored in the photosynthetic organisms. The second motivation for investigating thermodynamics is to separate the free energy into its enthalpy and entropy components, which provides more details and deeper understanding of the driving force of electron transfer mechanisms.

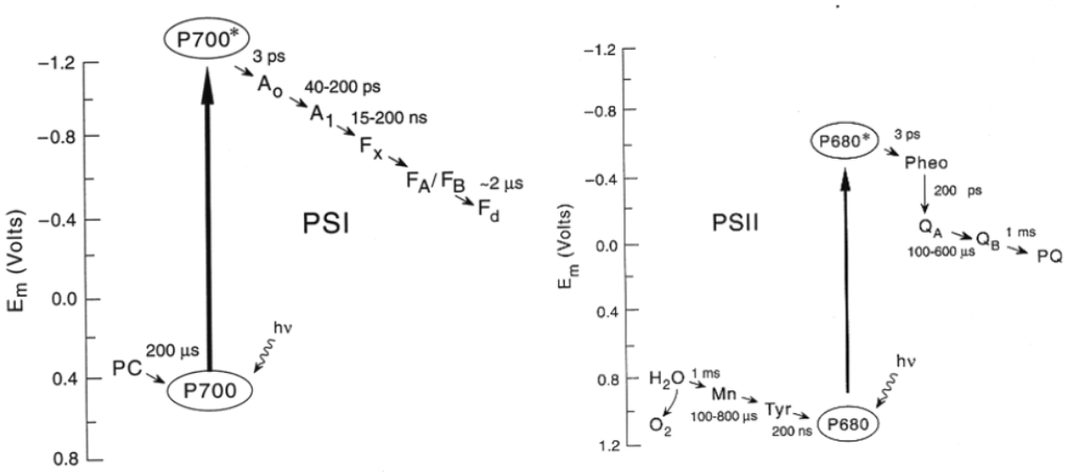

Fig. 4. Pathways and rates of electron transfer reactions in PS I (left panel) and PS II (right panel).

3. Principle of pulsed photoacoustics

Pulsed time-resolved photoacoustics provides an unique way to probe the molecular mechanism of electron transfer and proton transfer events in chemical reactions (Braslavsky & Heibel, 1992; Chen & Dibold, 1996; Borsarelli & Braslavsky, 1999; Feitelson & Mauzerall,

2002; Andres et al., 2006; Crovetto et al., 2006; Davies et al., 2008) and photosynthetic systems (Malkin, 2000; Herbert et al., 2001; Delosme, 2003; Mauzerall, 2006). For a given photoreaction, the accessible parameters include the molecular volume change secondary to conformational change or electrostriction, and enthalpy changes. With the measurement of enthalpy change by pulsed photoacoustics, the reaction entropy can be calculated when free energy is known (Feitelson & Mauzerall, 1996; Edens et al., 2000; Hou & Mauzerall, 2006).

3.1 Molecular volume change by electrostriction and structural conformational changes

Figure 3 shows the experimental setup of the pulsed photoacoustic apparatus, which enables one to determine the volume change and enthalpy of photoreactions on the nanosecond to microsecond time scales. A Nd:YAG laser and OPO are used to produce light of 680 nm and 700 nm with 1-mm light path. Consider the different response time of film, the PA detector containing a 128 mm piezoelectric film and 1-cm thickness of cell are used for the microsecond time scale photoacoustic experiments. A 28 μm film and 1-mm path cell are used for the nanosecond measurements. A 5-cm dielectric mirror was used according to the design of Arnaut *et al.* (Arnaut et al., 1992).

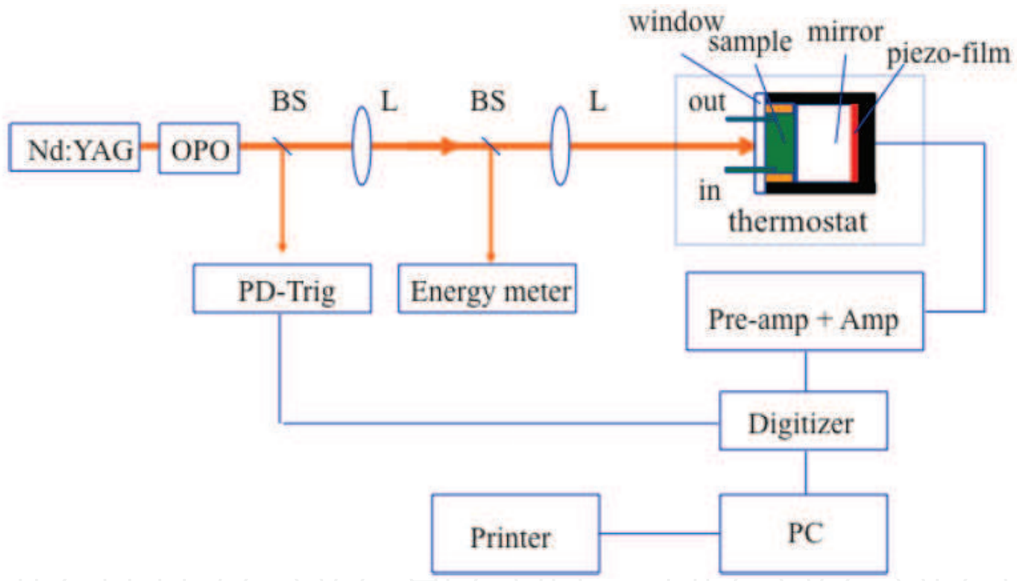

Fig. 3. Block diagram of pulsed photoacoustic system on the nanosecond-microsecond time scale. BS = beam splitter, L = lens, Amp = amplifier, OPO = optical parametric oscillator.

The advantage of using the mirror in the photoacoustic system is two-fold: (1) to increase light absorption and (2) to generate the time delay to eliminate the electric artifact in photoacoustic measurements. The volume change or heat of a photochemical reaction generates a pressure in a photoacoustic cell. The pressure is sensed by a piezo film or a microphone and recorded as a form of sound wave, designed photoaoustic wave or photoacoustic signal. To calibrate the photoacoustic signal, a reference must be used. A photoacoustic reference is a sample that degrades all the absorbed energy to heat within the resolving time interval of the apparatus. Two kinds of photoacoustic references are used to ensure the accuracy of the experimental data. The first is an external black ink reference, which is the supernatant fraction of high-quality commercial black carbon ink suspension

after centrifugation. The other is an internal reference—the light-saturated photosynthetic material. The photoacoustic signal generated by a reference is described by Equation 1:

$$PA_{ref} = \frac{F \cdot \alpha'}{\kappa} E_a \cdot I(t) \tag{1}$$

where E_a is photon energy absorbed by the sample, F is piezo film sensitivity, α′ is an abbreviation for thermal expansivity/heat capacity ‘ density, k is compressibility, and $I(t)$ is the impulse response of the system.

The photoacoustic signal is produced by the active photosynthetic reaction centers, which form a charge-separated radical pair upon light excitation, which undergo light-induced structural conformational change. The signal typically consists of two components (Equation 2).

$$PA_{RC} = \frac{F}{\kappa}\left[\alpha' \cdot Q_{RC} + \Delta V_{RC}\right] \cdot I(t) \tag{2}$$

where Q_{RC} is the heat output, which includes the enthalpy change of the reaction and other rapidly released heat, and DV_{RC} is the molecular volume change of the reaction.

When the temperature of the sample in aqueous solution is above the maximum density temperature (~4 °C), the heat output (Q_{RC}) of a photochemical reaction induces the volume expansion of solution. When the temperature is below ~4 °C, the heat induces the volume contraction. At ~4 °C, the heat component (Q_{RC}) is zero as the expansibility of water is zero. The photoacoustic signal at ~4 °C is simply the molecular volume change (ΔV_{RC}). To determine the precise values of the volume change resulting from charge separation in the photosynthetic materials, two different approaches are used: (1) volume yield measurements, and (2) saturation measurements.

In the first approach, the flash yield ($\Delta V/E$) is the volume change per unit photon energy absorbed by the system. The flash yield of the photoacoustic (DV/E) signal is dependent on the excitation photon flux, following Equation (3):

$$\frac{\Delta V_{RC}}{E} = N\Delta V_Y \frac{(1 - e^{\Phi\sigma E})}{N\sigma E} \tag{3}$$

Assuming ΔV does not change over a small temperature range, ΔV_{RC} is obtained in the limiting low pulse energy region (the linear region of Equation 3) by normalizing to the reference photoacoustic signal, converting PA_{ref} to volume *via* a′ at 25 °C and correcting for the change in the compressibility of water between T_m and 25 °C:

$$\Delta V_{RC} = \frac{PA_{RC}^{Tm}}{PA_{ref}^{25}} \times \frac{\kappa^{Tm}}{\kappa^{25}} \times \Delta V_{ref} \tag{4}$$

where DV_{ref} = α′E, is the thermal volume change of the reference at its temperature. Since the system is linear, one can calculate ΔV_{ref}, the thermal volume change at 25 °C, for each absorbed photon at the excitation wavelength. At low energy, one obtains the volume per center multiplied by the quantum yield, $\Phi \cdot \Delta V_y$. However, if the energy is too low, the photoacoustic signal-to-noise ratio is poor. In the case of photosynthetic reaction centers the value of volume change can be obtained by fitting a curve to Equation 3 and extrapolating to zero excitation energy.

In the second approach, every photosynthetic reaction center is excited to obtain the maximum photoacoustic signal. Fitting of the photoacoustic data to Equation 5 allows one to obtain the light saturated volume change, ΔV_s:

$$\Delta V = N\Delta V_s(1 - e^{-\Phi\sigma E}) \tag{5}$$

where ΔV_S is the volume change produced per photosynthetic reaction center; s is the optical cross section per photosynthetic reaction center; Φ is the quantum yield of the photochemical reaction, and E is the excitation photon flux.

In this method, one must calculate the number of photosynthetic reaction centers in the illuminated volume of the cell (~0.34 mL), N, to obtain the real volume change ΔV_s. The effective cross-section ($\Phi\cdot\sigma$) can also be obtained from the fit of the curves. This approach measures the absolute number of photosynthetic centers, calculated without assumptions of the quantum yield assuming all centers are successfully "hit" with enough energy. Although these two methods use the same set of data, the calculation of ΔV is differently weighted and completely different.

3.2 Quantum yield of photoreaction

The photoacoustic measurement includes the enthalpy or volume changes times the quantum yield, which can be determined using the light saturation curve of photoacoustics. The light saturation function at 4 °C (where there is no thermal signal) contains the photochemical quantum yield. For a simple system with one cross section, the photoacoustic signal is described by the cumulative one-hit Poisson distribution (Equation 6).

$$PA = N \cdot PA_0(1 - e^{-\Phi\cdot\sigma\cdot E}) \tag{6}$$

where N is the numbers of centers in the sample, PA_0 is the photoacoustic signal produced per successful hit of the reaction centers; s and Fs are the optical cross section and effective optical cross section; F is the quantum yield, E is the photon energy absorbed by the sample, and A is the absorbancy of solution.

The effective cross section can be obtained by the curve fit of the photoacoustic saturation curve. As the optical cross section, s with units of area per reaction center, can be calculated from the chlorophyll content and ratio of chlorophyll to the primary electron donor, the quantum yield of chemistry can be determined.

3.3 Enthalpy and entropy changes of photoreaction

The enthalpy change of electron transfer reactions in photosynthetic reaction centers can be calculated by the Equation 7:

$$\Delta H = (E_{h\nu} - E_{trap}) - \frac{\left(\frac{d(PA\cdot\kappa)_{RC}}{d\alpha}\right)}{\left(\frac{d(PA\cdot\kappa)_{ref}}{d\alpha}\right)} \times E_{h\nu} \tag{7}$$

As discussed above, pulsed photoacoustics directly measures the enthalpy and volume changes of the reactions on the nanosecond and microsecond time scales. With the given free energy, the entropy change is calculated from $\Delta G = \Delta H - T\Delta S$.

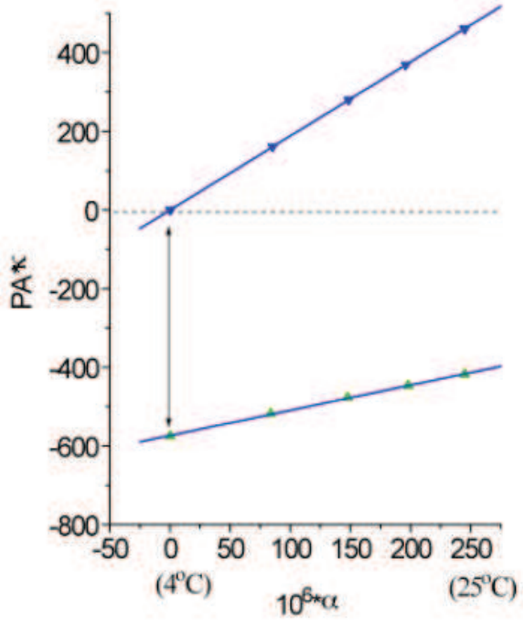

Fig. 4. Typical plot of the product of the photoacoustic signal and water compressibility (k) versus water expansivity (a) for ink reference (blue symbols) and PS I complex (green symbols).

To determine the reaction enthalpy and volume changes, the photoacoustic waves of ink references and photoactive samples such as PS I complexes are recorded at five temperatures, 4, 10, 15, 20, and 25 °C. A typical data analysis is plotted in the product of the photoacoustic intensity (peak to peak value) and water compressibility versus the water expansivity (Figure 4). The deconvolution analysis on photoacoustic waves allows one to time-resolve the thermodynamic parameters of each individual step of photoreaction (Rudzki et al., 1985; Feitelson & Mauzerall, 1996, 2002). The photoacoustic pressure wave is caused by the rate of the heat release. The two or more steps of a photochemical reaction will change the shape (wider or narrower) of photoacoustic wave than the photoacoustic reference. The linear fit of the experimental points gives intercept and slope of ink reference and PS I samples, respectively. The molecular volume change of PS I on the 1 μs time scale can be easily obtained by inserting the intercepts values of the linear fit of ink reference and PS I sample to the Equation 4. The enthalpy change of the photochemical reaction in PS I on the 1 μs time scale may be found *via* the Equation 7 using the slopes of the fit.

4. Enthalpy, entropy, and volume changes of photosynthetic reactions

The pulsed photoacoustic technique gives a direct measurement of the enthalpy change of photosynthetic electron transfer reactions (Feitelson & Mauzerall, 1996; Edens et al., 2000). A microphone may detect the photoacoustic waves *via* the thermal expansion in the gas phase. The 50-fold larger thermal expansion of a gas over liquid makes the microphone more sensitive. A gas-coupled microphone in a closed chamber is used as a detector on the ms time scale. This method allows measurements of the photosynthetic thermal efficiency, or energy storage, and of the optical cross-section of the light harvesting systems (Canaani et al., 1984; Mauzerall, 1990; Braslavsky & Heibel, 1992). However, the time resolution is low,

typically about 30 μs, and inappropriate for obtain thermodynamic parameters on the microsecond and nanosecond time scales. The use of piezoelectric films acoustically coupled to a liquid sample and a pulsed laser light source increased the time resolution of the photoacoustic technique to the microsecond scale (Nitsch et al., 1988; Mauzerall et al., 1995). Photoacoustic thermodynamic studies have been carried out on isolated photosynthetic reaction centers from bacteria *Rb. sphaeroides* (Arata & Parson, 1981), on PS I from cyanobacteria (Delosme et al., 1994), and on PS II from spinach and *Chlamydomonas reinhardtii* (Delosme et al., 1994).

Measuring the energetics of photobiological reactions *in vivo* is of more interest because the local environment of photosystems may exert a prevailing consequence on their kinetics and thermodynamics. Pulsed photoacoustics *via* a microphone detector revealed the oxygen evolution and oxygen uptake *in vivo* on the millisecond time scale (Mauzerall, 1990). Using a piezo film detector, the *in vivo* enthalpy and volume changes of photosystem I and photosystem II of *Synechocysits sp. PCC 6803* were obtained on the microsecond time scale (Hou et al., 2001; Hou et al., 2001). The contribution of the two photosystems was distinguished by excitation at two different wavelengths, 625 nm for predominant excitation of PS I and 680 nm for PS II, respectively. The difficulty in the photoacoustic measurements of intact cells is the heterogeneous or "cell" artifact at the temperature of maximum density of near 4 °C. To correct the "cell" artifact, five measurements are needed instead of usual three (see reference (Hou et al., 2001) for details). The enthalpy and volume changes of intact cells of *Synechocystis sp. PCC 6803* were in good agreement with those of isolated complexes within the experimental errors.

Theoretical calculations of electron transfer have often assumed the reaction entropy to be zero. For example, the standard formulation of Marcus theory assumes that the vibrations coupled to electron transfer have the same frequency in the reactant and product states (Marcus & Sutin, 1985). Marcus theory introduces reorganization energy to interpret the reaction rate of electron transfer reactions. The reorganization energy can have two contributions: a vibration term and a solvent term. Treatments of the temperature dependence of the rate of electron transfer often assume that the free energy is independent of temperature (Gunner & Dutton, 1989). However, these assumptions are called into question by recent work. For instance, the entropy change often neglected in an artificial photosynthetic system was actually determined to be large (Rizzi et al., 2008). A fit of Marcus reorganization energy cannot interpret the observed volume change of electron transfer reaction.

Using pulsed photoacoustics, the volume change and enthalpy of electron transfer reaction were measured in aqueous solution (Feitelson & Mauzerall, 1996) and in the photosynthetic reaction center complex of *Rb. sphaeroides* (Edens et al., 2000). A large entropy was calculated based on these measurements. Further photoacoustic measurements revealed that the entropy change of electron transfer in PS I trimer from *Synechocystis* sp. PCC 6803 on the microsecond time scale was the same as that in bacterial centers (Hou et al., 2001). The volume contraction of reaction centers of PS I, which results directly from the light-induced charge separation forming $P_{700}{}^{+}F_A/F_B{}^{-}$ from the excited state $P_{700}{}^{*}$, was determined to be −26 $Å^3$. The enthalpy of the above electron transfer reaction was found to be −0.39 eV. Taking the free energy of the above reaction as the difference of their redox potentials *in situ* allows one to calculate an apparent entropy change ($T\Delta S$) of +0.35 eV. In contrast, electron transfer in PS II core complexes from *Synechocystis* sp. PCC 6803 is accompanied by a small negative entropy change (Hou et al., 2001). At pH 6.0, the volume contraction of PS II was

determined to be −9 Å^3, and the enthalpy change −0.9 eV for the formation of the state $P_{680}^+Q_A^-$ from P_{680}*. The ΔV of PS II, smaller than that of PS I and bacterial centers, is assigned to electrostriction and analyzed using the Drude-Nernst equation. To explain the small ΔV for the formation of $P_{680}^+Q_A^-$ or $Y_Z^\bullet Q_A^-$ we proposed that fast proton transfer into a polar region is involved in this reaction. These observations were confirmed using intact living cells of the same organism (Boichenko et al., 2001). These thermodynamic parameters are summarized in Figure 5. The enthalpies for the formation of states $P_{700}^+F_{AB}^-$ from P_{700}* and $Y_Z^\bullet P_{680}Q_A^-$ from P_{680}* *in vivo* were estimated to be about −0.3 eV and −1 eV, respectively. Comparison of these values with the free energies of the reactions indicates a significant contribution of the apparent entropy changes $T\Delta S$, +0.4 and −0.24 eV for the formation of ion-radical pairs in PS I and PS II, respectively.

In order to obtain detailed information on intermediates in the PS I reactions, we measured the volume change and enthalpy change on the nanosecond time scale. The time constant of charge transfer from A_1^- to $F_{A/B}$ is reported to be 20 to 200 ns (Brettel & Leibl, 2001). However the modeling analysis of the electron transfer reactions in PS I by electron

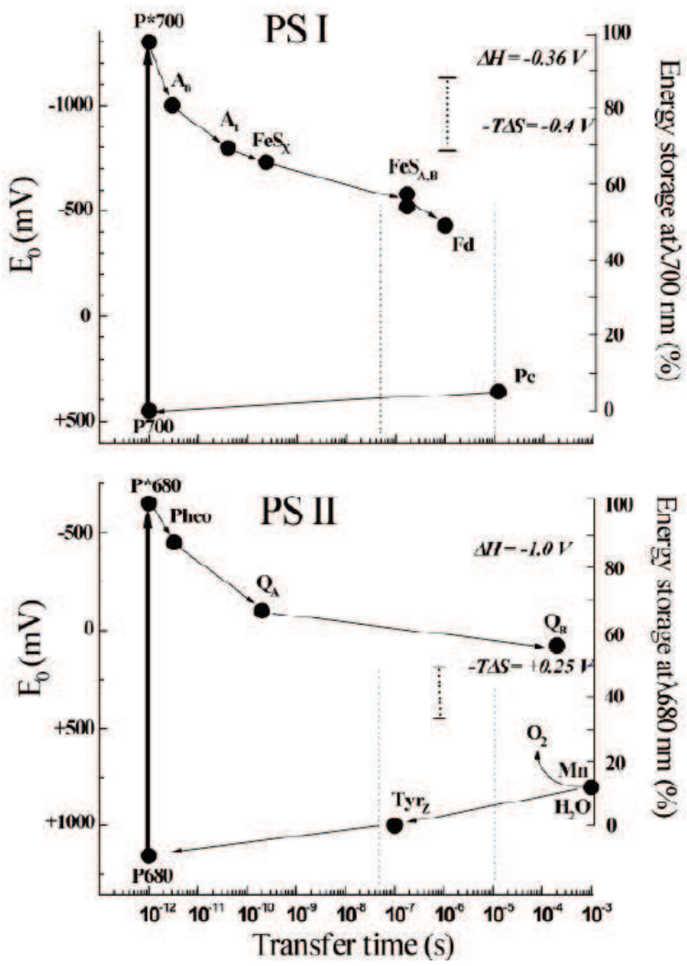

Fig. 5. Energetic scheme of PS I and PS II. Dashed lines show the time window of the PA measurements (reproduced with permission from the American Chemical Society (Boichenko et al., 2001)).

tunneling theory indicate complex equilibria between the various species (Santabarbara et al., 2005). The enthalpy and volume changes associated with this reaction and with the charge separation of the $P_{700}^* \rightarrow A_1$ reaction seem unknown. The photoacoustic waves of PS I may involve the contributions of the initial and subsequent electron transfer reactions (Figure 4). The deconvolution of the time derivative of the volume or heat release function with the apparatus response function provided by the reference signal enables us to resolve the fast and slow photoacoustic components (Feitelson & Mauzerall, 1996; Zhang & Mauzerall, 1996; Strassburger et al., 1997). It is possible to time-resolve the thermodynamic parameters of individual steps in PS I by the deconvolution analysis.

As shown in Figure 6, deconvolution analysis of photoacoustic signals on microsecond time scales resolves enthalpy and volume changes of two steps: (1) a prompt component (<10 ns)

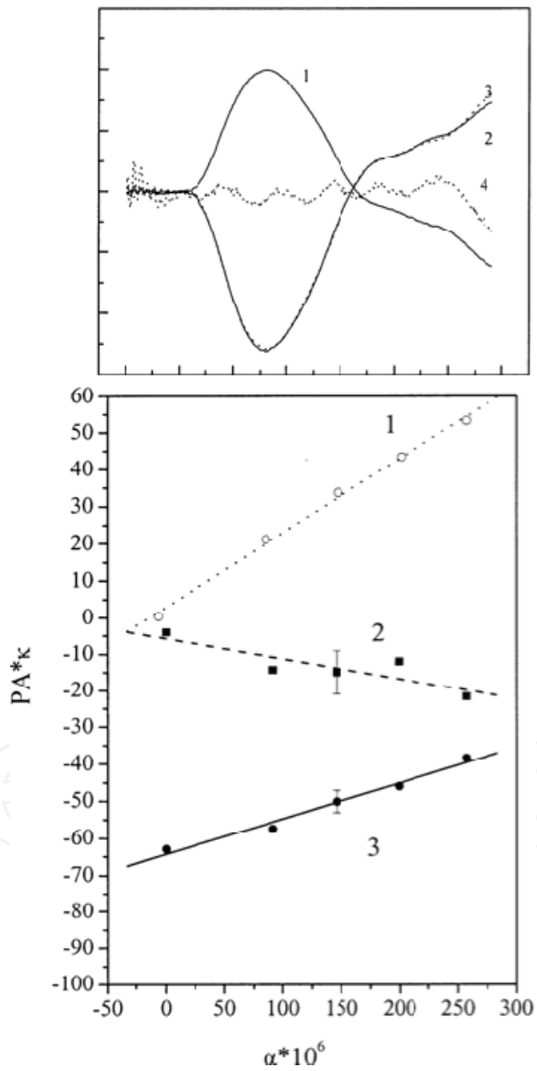

Fig. 6. Deconvolution analysis of a typical photoacoustic pressure wave to time-resolve the enthalpy and volume changes of two individual electron transfer steps in PS I of *Synechocystis* sp. PCC 6803 (reproduced with permission from the American Chemical Society (Hou & Mauzerall, 2006)).

with large negative enthalpy change (−0.8 ± 0.1 eV) and large volume change (−23 ± 2 A^3), which are assigned to the $P_{700}^* \rightarrow A_1^- F_X$ step, and (2) a component with ~200 ns lifetime, which has a positive enthalpy change (+0.4 ± 0.2 eV) and a small volume change (−3 ± 2 A^3) which are attributed to the $A_1^- F_X \rightarrow F_{A/B}^-$ step. This parameters were confirmed by a similar analytsis of photoacoustic waves on the nanosecond time scale. For the fast reaction using the redox potentials of A_1F_X (−0.67 V) and P_{700} (+0.45 V) and the energy of P_{700}^* (1.77 eV), the free energy change for the $P_{700}^* \rightarrow A_1^- F_X$ step is −0.63 eV. Thus, the entropy change ($T\Delta S$, T = 25 °C) is −0.2 ± 0.3 eV. For the slow reaction, $A_1^- F_X \rightarrow F_{A/B}^-$, taking the free energy of −0.14 eV (Santabarbara et al., 2005), the entropy change ($T\Delta S$) is positive, (+0.54 ± 0.3 eV). The redox thermodynamics of many FeS proteins (ferrodoxins) have been determined. Interestingly, most of the $Fe_4S_4(Cys)_4$ proteins have positive enthalpies of reduction of +0.3 to +0.4 eV, while the others have very small negative enthalpies. The authors explain the enthalpies in terms of electrostatic interactions with the protein dipoles. All the reduction entropies are negative as anticipated from the increase in charge and seem to vary in magnitude opposite to the enthalpies. Thus the positive enthalpy of the $A_1^- F_X$ to $F_{A/B}$ reaction may be assigned in part to the FeS cluster reduction. The positive entropy may have contributions from the freeing of oriented polar groups on quinone anion oxidation. The previous step has negative entropy as expected.

To understand more details of electron transfer thermodynamics, it is of interesting to determine the thermodynamic parameters of electron transfer in the photosynthetic electron transfer mutants on both the nanosecond and microsecond time scales. It has been generally believed that phylloquinone is difficult to dislodge from the A_1 binding site in PS I, in contrast to the ubiquinone (Q_A) in bacterial centers from *Rb. Sphaeroides* that can be easily replaced by a wide variety of different quinones (Gunner & Dutton, 1989; Xu & Gunner, 2001). A biological method to remove phylloquinone was recently devised. Targeted inactivation of the *menA* and *menB* genes that code for phytyl transferase and napthoate synthase in the phylloquinone biosynthetic pathway (Johnson et al., 2000) precludes its availability for incorporation in the A_1 site. Yet, in spite of the demonstrated absence of phylloquinone, the *menA* and *menB* null mutants grow photosynthetically. EPR measurements show that plastoquinone-9 (A_P) is recruited into the A_1 site (Johnson et al., 2000)and functions as an efficient 1-electron electron carrier (Zybailov et al., 2000). Time-resolved optical studies indicate the forward electron transfer from A_1^- to F_X is slowed 1000-fold, to 15 and 300 µs, compared to 20 and 200 ns in wild-type PS I (Semenov et al., 2001). Given the altered kinetics of electron transfer, it will be of interest to investigate the effect of these mutations on the thermodynamics of electron transfer in PS I. These thermodynamic parameters reveal that the driving force in the photosynthetic reactions may be both enthalpic and entropic.

Figure 7 summarizes the volume changes, free energies, enthalpy and entropy changes on *menA/B* PS I in comparison with those on the wild-type PS I. Opened arrows are the early step forming $P_{700}^+A_1^-$ from P_{700}^* for the wild-type PS I or $P_{700}^+A_P^-$ from P_{700}^* for the mutants, and solid arrows are the number of the following reaction: $P_{700}^+A_P^- \rightarrow P_{700}^+F_{A/B}^-$. As shown in Panel A, the volume contraction of early step of photoreaction in the mutants (−17 $Å^3$) is smaller than that in the wild type (−21 $Å^3$). Similarly, the enthalpy change (−0.7 eV) of the early step in the mutants is smaller than that (−0.8 eV) in wild type PS I (Figure 7A and 7B). Assuming a redox potential of −0.6 V for plastoquinone-9 in the A_1 site (Semenov et al., 2001), the free energy (−0.7 eV) of this early reaction in the mutants is larger than the value

(−0.6 eV) in the wild type as indicated in Figure 7C. Taking the difference of free energy and enthalpy change in the mutants, the apparent entropy change of the early step in mutants is zero. In contrast, the apparent entropy change in the wild-type PS I is calculated to be +0.2 eV. Since the apparent entropy change for the overall reaction of the generation of P_{700}^{+} $F_{A/B}^{-}$ from P_{700}^{*} is +0.35 eV (Hou et al., 2001), it implies that the latter reaction in the mutants, *i.e.*, the P_{700}^{+} A_P^{-} $F_{A/B}$ → P_{700}^{+} A_P $F_{A/B}^{-}$ reaction, is almost completely entropy-driven (TΔS = +0.4 eV and ΔG= −0.1 eV) (Figure 7D). Therefore, based on our experimental results we propose that the foreign quinone (A_P) in PS I does affect the thermodynamics of charge separation in the early steps in PS I with a smaller volume and enthalpy changes, a large free energy and zero entropy change.

The observed thermodynamic data of the *menA* and *menB* null mutants show little difference. This is expected because the recruited quinone (A_P) is the same in both mutants. Volume change of mutant PS I following charge separation on both time scales is −16 ± 2 Å^3. The quantum yield of charge separation in PS I of the mutants is slightly lower (85 ± 10%) than that of the wild-type PS I (96 ± 10%). The observed reaction is assigned to the formation of $P_{700}^{+}A_P^{-}$ $F_{A/B}$ from $P_{700}^{*}A_P$ $F_{A/B}$. The enthalpy change (ΔH) of about −0.69 ± 0.1 eV in mutant PS I was obtained for this reaction. In contrast, a large enthalpy change of ~ −1.0 eV for the formation of $P_{700}^{+}A_1^{-}$ from P_{700}^{*} in the wild-type PS I was observed. These results strongly suggest that not only the kinetics but also the thermodynamics of electron transfer reactions in PS I is significantly affected by the recruitment of the foreign plastoquinone-9 into the A_1 site (Hou et al., 2009).

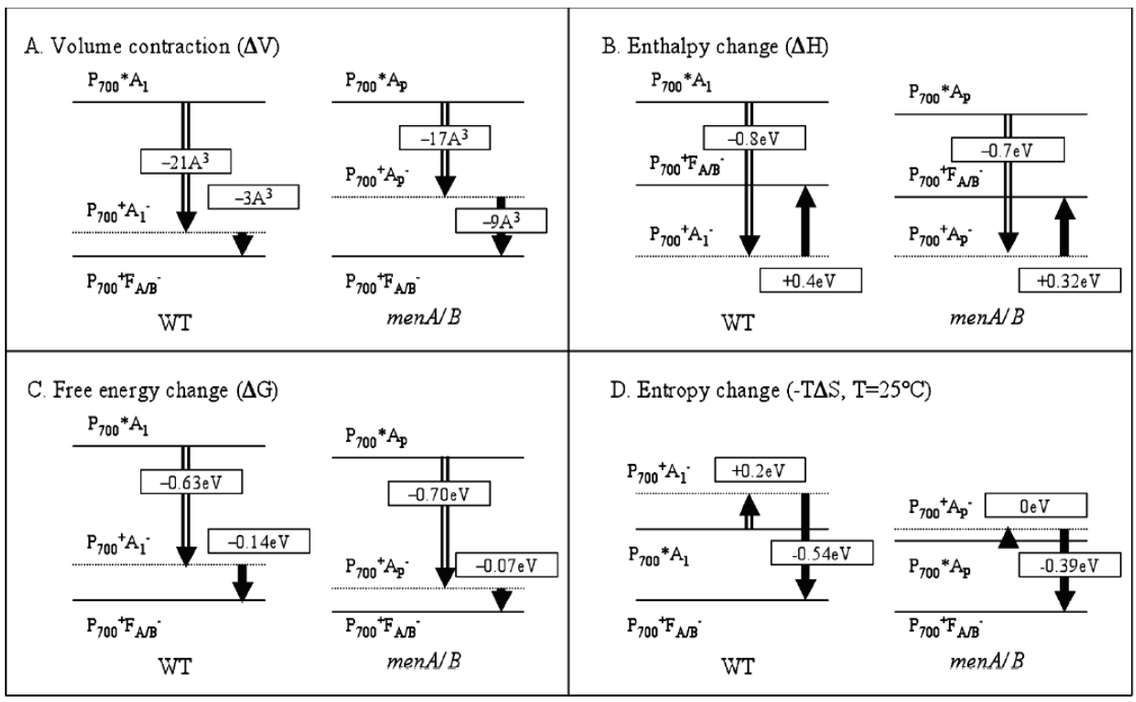

Fig. 7. Thermodynamic parameters of charge separation in *menA/B* PS I and wild-type PS I from *Synechocystis* 6803 (reproduced with permission from the American Chemical Society (Hou et al., 2009)).

5. Limitations and possible solutions

The thermodynamic parameters of electron transfer in photosynthetic reaction center complexes and in whole cells of *Synechocystis* have been determined using pulsed photoacoustics (Boichenko et al., 2001; Hou et al., 2001; Hou et al., 2001). However, the parameters in *Synechocystis* PS II were inconsistent with those obtained using *Chlamydomonas* and spinach chloroplast (De Vitry et al., 1991; Delosme et al., 1994)). The *in vitro* measurements, in particular, showed a significant difference from the *in vivo* values. These discrepancies in purified complexes from different organisms such as *Synechocystis*, *Chlamydomonas*, and spinach chloroplasts must be clarified.

We previously determined the volume changes and enthalpy changes of electron transfer in *Synechocystis* PS I complexes on the microsecond time scale (Hou et al., 2001) and then time-resolved two individual steps in the complexes on the nanosecond time scale (Hou & Mauzerall, 2006). A significant entropic component was found. In future work, we intend to determine the thermodynamic parameters in PS I *in vitro* and *in vivo* using photosynthetic electron transfer mutants to uncover the roles of the protein matrix in electron transfer steps.

In contrast, for the volume changes in PS I and bacterial reaction centers with an reasonable number within the error margins, the volume change of PS II charge separation is in the range from −2 to −16 $Å^3$ (Hou et al., 2001). For example, Boichenko *et al.* (Boichenko et al., 2001) reported a −2 $Å^3$ in the whole cells of cyanobacterium *Synechocystis*, and Delosme *et al.* (Delosme, 2003) observed −9 $Å^3$ from *Chlamydomonas* to −16 $Å^3$ from spinach. This obvious inconsistency needs to be investigated and clarified. The pH, species of organisms, redox potentials of electron donor/acceptors, and cell artifacts in the photoacoustic measurements may cause the discrepancy.

The discrepancy might arise from the fact that the measurements were performed at different pH values. The volume change of our previous photoacoustic measurements showed a strong pH dependence of volume change in PS II core complexes. A volume change of −3 $Å^3$ was observed at pH 9.0 and −9 $Å^3$ at pH 6.0 (Hou et al., 2001). Future work may determine the volume change of charge separation in PS II complexes using our previous photoacoustic procedures over a range of pH. The volume change will be measured by the yield and saturation method, respectively. As Delosme et al. pointed out, the discrepancy of the volume change may be due to the use of different organisms: cyanobacteria *versus* green plants (Delosme, 2003). We will test this possibility by using the photosystem II preparations from cyanobacteria, green algae, and higher plants. These PS II preparations can be purified from cyanobacterium *Synechocystis* 6803, from green algae *Chlamydomonas reinhardii*, and from spinach chloroplasts following our established method (Hou et al., 2000). The volume change of charge separation in PS II should be determined and evaluated against the data from different groups.

The inconsistency in volume changes and enthalpies of electron transfer could be due to the difference in intactness: *in vitro versus in vivo*. Most of the *in vitro* preparations gave around −10 $Å^3$ compared to −2 $Å^3$ for the *in vivo* system. A number of factors *in vivo* are different from the *in vitro* preparations. The overlap of absorption of PS I and PS II in the whole cell preparations is significant. We estimated 30% PS II contributions and 70% PS I at 625 nm. In contrast, the contribution of PS I is 20% PS I and of PS II is 80% at 690 nm, respectively (Boichenko et al., 2001). Use of the PS I-depleted mutant may be required to address this problem. Based on preliminary unpublished data Delosme *et al.* argued that the thermal efficiency of purified PS II core from *Thermosynechococcus elongatus* strongly depends on the

experimental conditions (Delosme, 2003), such as the electron donor or acceptor used, and could be significantly higher than our previous data. This discrepancy needs to be clarified.
A number of photosynthetic electron transfer mutants in addition to chemically modified the reaction centers altered the kinetics of photosynthetic reactions. For example, the photosynthetic electron transfer mutants, including *menA*, *menB*, and *menG* null PS I mutants and A_0 to F_X, F_A, and F_B mutants, are available. Pulsed photoacoustics may probe these mutants to explore the effects of mutation on thermodynamic parameters of electron transfer in PS I. The focus should be placed on the effects of the mutations on thermodynamics of photoreactions in photosynthesis. However, the entropic contribution may suffer from the limited published data reporting free energy values. To overcome these obstacles, the electrochemical measurements to determine the redox potentials *in situ* and computational study to calculate the redox potentials of the cofactors will be beneficial.
It has been a long-term goal to reveal the thermodynamics of PS II oxygen evolution. However, the time window of current photoacoustics is on the microsecond time scale, which is too fast to determine the millisecond step of PS II oxygen evolution cycle. Recently, using photothermal beam deflection techniques the enthalpies of PS II water oxidation were reported (Krivanek et al., 2008). Using a novel photopressure cell that enables one to obtain the volume and enthalpy changes on the microsecond to second time scales (Liu et al., 2008), the thermodynamic parameter of reactions involved in PS II oxygen evolution might be determined.

6. Conclusion

To fully understand a chemical reaction, it is necessary to understand not just its kinetics, but also its thermodynamic parameters. However, in contrast to the kinetics of electron transfer mechanisms, thermodynamic information is far less accessible. The driving force of the chemical reaction is the Gibbs free energy, which is composed of enthalpic and entropic components. The theory of electron transfer in chemical and biological system was developed by Marcus (Marcus & Sutin, 1985) and played a key role in advancing the understanding electron transfer mechanisms, including photosynthetic systems (Turro et al., 1996; Renger et al., 1998; Mayer et al., 2006; LeBard et al., 2008). However, one weakness of the theory is the omission of entropic contribution in the electron transfer steps.
The recent experimental results pointed out the crucial role of entropy change in chemical and biological systems (Feitelson & Mauzerall, 1996; Edens et al., 2000; Xu & Gunner, 2000; Crovetto et al., 2006; Hou & Mauzerall, 2006). The follow-up and extensive thermodynamic measurements especially by photoacoustics is worth while. Pulsed photoacoustics provides novel insights on the entropic contribution to electron transfer in proteins and is able to probe the role of the membrane environment and cofactors *in vitro* and *in vivo* in terms of a broadly thermodynamic view. These unique features of photoacoutstics studies provide the potential for a deeper understanding of the mechanisms of electron transfer and proton-coupled electron transfer in chemical and biological systems. They also provide a framework to modify and improve the existing Marcus electron transfer theory as well as the formulation of a comprehensive electron transfer theory. The results of photoacoustics experiments also provide direct information about the function of membrane proteins central to photosynthesis. In particular, the photosynthetic membrane proteins are excellent models for elucidating electron transfer and proton transfer mechanism in other membrane proteins.

7. References

Amunts A, Drory O, Nelson N (2007) The structure of a plant photosystem I supercomplex at 3.4 A resolution. Nature 447: 58-63

Andres GO, Martinez-Junza V, Crovetto L, Braslavsky SE (2006) Photoinduced Electron Transfer from Tetrasulfonated Porphyrin to Benzoquinone Revisited. The Structural Volume-Normalized Entropy Change Correlates with Marcus Reorganization Energy. J Phys Chem A 110: 10185-10190

Arata H, Parson WW (1981) Enthalpy and volume changes accompanying electron transfer from P-870 to quinones in *Rhodopseudomonas sphaeroides* reaction centers. Biochim Biophys Acta, 636: 70-81

Arnaut LG, Caldwell RA, Elbert JE, Melton LA (1992) Recent advances in photoacoustic calorimetry: theoretical basis and improvements in experimental design. Rev Sci Instrum 63: 5381-5389

Boichenko VA, Hou J-M, Mauzerall D (2001) Thermodynamics of Electron Transfer in Oxygenic Photosynthetic Reaction Centers: Volume Change, Enthalpy, and Entropy of Electron-Transfer Reactions in the Intact Cells of the Cyanobacterium *Synechocystis* PCC 6803. Biochemistry 40: 7126-7132

Borsarelli CD, Braslavsky SE (1999) Enthalpy, Volume, and Entropy Changes Associated with the Electron Transfer Reaction between the 3MLCT State of $Ru(Bpy)_3^{2+}$ and Methyl Viologen Cation in Aqueous Solutions. J Phys Chem A 103: 1719-1727

Braslavsky SE, Heibel GE (1992) Time-resolved photothermal and photoacoustic methods applied to photoinduced processes in solution. Chem Rev 92: 1381-1410

Brettel K (1997) Electron transfer and arrangement of the redox cofactors in photosystem I. Biochim Biophys Acta, 1318: 322-373

Brettel K, Leibl W (2001) Electron transfer in photosystem I. Biochim Biophys Acta 1507: 100-114

Canaani O, Barber J, Malkin S (1984) Evidence that phosphorylation and dephosphorylation regulate the distribution of excitation energy between the two photosystems of photosynthesis in vivo: Photoacoustic and fluorimetric study of an intact leaf. Proc Natl Acad Sci U S A 81: 1614-1618

Chen, H.X.; Dibold, G. (1996) Production of the photoacoustic effect and transient gratings by molecular volume changes. J Chem Phys, *104*, 6730-6741.

Crovetto L, Martinez-Junza V, Braslavsky SE (2006) Entropy changes drive the electron transfer reaction of triplet flavin mononucleotide from aromatic amino acids in cation-organized aqueous media. A laser-induced optoacoustic study. Photochem Photobiol 82: 281-290

Davies KW, Maivald D, Grabowski JJ (2008) A photoacoustic calorimetric characterization of the reaction enthalpy and volume for the preparation of a reactive intermediate from $CpMn(CO)_3$. J Photochem Photobiol A 197: 335-341

De Vitry C, Diner BA, Popot JL (1991) Photosystem II particles from *Chlamydomonas reinhardtii*. Purification, molecular weight, small subunit composition, and protein phosphorylation. J Biol Chem 266: 16614-16621

Dekker JP, Van Grondelle R (2000) Primary charge separation in Photosystem II. Photosynth Res 63: 195-208

Delosme R (2003) On some aspects of photosynthesis revealed by photoacoustic studies: a critical evaluation. Photosynth Res 76: 289-301

Delosme R, Beal D, Joliot P (1994) Photoacoustic detection of flash-induced charge separation in photosynthetic systems. Spectral dependence of the quantum yield. Biochim Biophys Acta, 1185: 56-64

Edens GJ, Gunner MR, Xu Q, Mauzerall D (2000) The Enthalpy and Entropy of Reaction for Formation of $P^+Q_A^-$ from Excited Reaction Centers of *Rhodobacter sphaeroides*. J Am Chem Soc 122: 1479-1485

Feitelson J, Mauzerall D (1996) Photoacoustic Evaluation of Volume and Entropy Changes in Energy and Electron Transfer. Triplet State Porphyrin with Oxygen and Naphthoquinone-2-Sulfonate. J Phys Chem 100: 7698-7703

Feitelson J, Mauzerall D (2002) Enthalpy and Electrostriction in the Electron-Transfer Reaction between Triplet Zinc Uroporphyrin and Ferricyanide. J Phys Chem B 106: 9674-9678

Ferreira KN, Iverson TM, Maghlaoui K, Barber J, Iwata S (2004) Architecture of the photosynthetic oxygen-evolving center. Science 303: 1831-1838

Gobets B, van Grondelle R (2001) Energy transfer and trapping in photosystem I. Biochim Biophys Acta 1507: 80-99

Gunner MR, Dutton PL (1989) Temperature and $\Delta G°$ dependence of the electron transfer from BPh^- to Q_A in reaction center protein from *Rhodobacter sphaeroides* with different quinones as QA. J Am Chem Soc 111: 3400-3412

Herbert SK, Han T, Vogelmann TC (2001) New applications of photoacoustics to the study of photosynthesis. Photosynth Res 66: 13-31

Hou HJM, Mauzerall D (2006) The $A\text{-}F_X$ to $F_{A/B}$ Step in *Synechocystis* 6803 Photosystem I Is Entropy Driven. J Am Chem Soc 128: 1580-1586

Hou HJM, Shen G, Boichenko VA, Golbeck JH, Mauzerall D (2009) Thermodynamics of Charge Separation of Photosystem I in the *menA* and *menB* Null Mutants of *Synechocystis* sp. PCC 6803 Determined by Pulsed Photoacoustics. Biochemistry 48: 1829-1837

Hou JM, Boichenko VA, Diner BA, Mauzerall D (2001) Thermodynamics of electron transfer in oxygenic photosynthetic reaction centers: Volume change, enthalpy, and entropy of electron transfer reactions in manganese-depleted photosystem II core complexes. Biochemistry 40: 7117-7125

Hou JM, Dejonghe D, Shan JX, Li LB, Kuang TY (2000) Orientation of pigments in the isolated photosystem II sub-core reaction center CP47/D1/D2/Cyt b-559 complexes: A linear dichroism study. J Integr Plant Biol 42: 1211-1214

Hou JM, Boichenko VA, Wang YC, Chitnis PR, Mauzerall D (2001) Thermodynamics of electron transfer in oxygenic photosynthetic reaction centers: a pulsed photoacoustic study of electron transfer in photosystem I reveals a similarity to bacterial reaction centers in both volume change and entropy. Biochemistry 40: 7109-7116

Johnson TW, Shen G, Zybailov B, Kolling D, Reategui R, Beauparlant S, Vassiliev IR, Bryant DA, Jones AD, Golbeck JH, Chitnis PR (2000) Recruitment of a foreign quinone into the A_1 site of photosystem I. I. Genetic and physiological characterization of phylloquinone biosynthetic pathway mutants in *Synechocystis* sp. pcc 6803. J Biol Chem 275: 8523-8530

Jordan P, Fromme P, Witt HT, Klukas O, Saenger W, Krauss N (2001) Three-dimensional structure of cyanobacterial photosystem I at 2.5 A resolution. Nature 411: 909-917

Krivanek R, Dau H, Haumann M (2008) Enthalpy changes during photosynthetic water oxidation tracked by time-resolved calorimetry using a photothermal beam deflection technique. Biophys J 94: 1890-1903

LeBard DN, Kapko V, Matyushov DV (2008) Energetics and kinetics of primary charge separation in bacterial photosynthesis. J. Phys. Chem. B 112: 10322-10342

Liu Y, Edens GJ, Grzymski J, Mauzerall D (2008) Volume and Enthalpy Changes of Proton Transfers in the Bacteriorhodopsin Photocycle Studied by Millisecond Time-Resolved Photopressure Measurements. Biochemistry 47: 7752-7761

Loll B, Kern J, Saenger W, Zouni A, Biesiadka J (2005) Towards complete cofactor arrangement in the 3.0 A resolution structure of photosystem II. Nature 438: 1040-1044

Malkin S (2000) The photoacoustic effect in leaves and its applications. Probing Photosynthesis: 484-524

Marcus RA, Sutin N (1985) Electron transfers in chemistry and biology. Biochim Biophys Acta, 811: 265-322

Mauzerall D (2006) Thermodynamics in photosystem I. In J. Golbeck (ed): Photosystem I: The Light-Driven Plastocyanin: Ferredoxin Oxidoreductase Vol 24: Springer, Dordrecht, pp 571-581

Mauzerall D, Feitelson J, Prince R (1995) Wide Band, Time-Resolved Photoacoustic Study of Electron Transfer Reactions: Difference between Measured Enthalpies and Redox Free Energies. J Phys Chem 99: 1090-1093

Mauzerall DC (1990) Determination of Oxygen Emission and Uptake in Leaves by Pulsed, Time Resolved Photoacoustics. Plant Physiol 94: 278-283

Mayer JM, Rhile IJ, Larsen FB, Mader EA, Markle TF, Dipasquale AG (2006) Models for Proton-coupled Electron Transfer in Photosystem II. Photosynth Res 87: 3-20

Nitsch C, Braslavsky SE, Schatz GH (1988) Laser-induced optoacoustic calorimetry of primary processes in isolated photosystem I and photosystem II particles. Biochim Biophys Acta, 934: 201-212

Renger G, Christen G, Karge M, Eckert HJ, Irrgang KD (1998) Application of the Marcus theory for analysis of the temperature dependence of the reactions leading to photosynthetic water oxidation: results and implications. J Biol Inorg Chem 3: 360-366

Rizzi AC, van Gastel M, Liddell PA, Palacios RE, Moore GF, Kodis G, Moore AL, Moore TA, Gust D, Braslavsky SE (2008) Entropic Changes Control the Charge Separation Process in Triads Mimicking Photosynthetic Charge Separation. J Phys Chem A 112: 4215-4223

Rudzki JE, Goodman JL, Peters KS (1985) Simultaneous determination of photoreaction dynamics and energetics using pulsed, time-resolved photoacoustic calorimetry. J Am Chem Soc 107: 7849-7854

Santabarbara S, Heathcote P, Evans MC (2005) Modelling of the electron transfer reactions in Photosystem I by electron tunnelling theory: the phylloquinones bound to the PsaA and the PsaB reaction center subunits of PS I are almost isoenergetic to the iron-sulfur cluster F_X. Biochim Biophys Acta 1708: 283-310

Semenov AY, Vassiliev IR, van Der Est A, Mamedov MD, Zybailov B, Shen G, Stehlik D, Diner BA, Chitnis PR, Golbeck JH (2001) Recruitment of a foreign quinone into the A_1 site of photosystem I. Altered kinetics of electron transfer in phylloquinone

biosynthetic pathway mutants studied by time-resolved optical, EPR, and electrometric techniques. J Biol Chem 275: 23429-23438

Strassburger JM, Gartner W, Braslavsky SE (1997) Volume and enthalpy changes after photoexcitation of bovine rhodopsin: laser-induced optoacoustic studies. Biophys J 72: 2294-2303

Turro C, Zaleski JM, Karabatsos YM, Nocera DG (1996) Bimolecular electron transfer in the Marcus inverted region. J Am Chem Soc 118: 6060-6067

Xu Q, Gunner MR (2000) Temperature Dependence of the Free Energy, Enthalpy, and Entropy of $P^+Q_A^-$ Charge Recombination in *Rhodobacter sphaeroides* R-26 Reaction Centers. J Phys Chem B 104: 8035-8043

Xu Q, Gunner MR (2001) Trapping Conformational Intermediate States in the Reaction Center Protein from Photosynthetic Bacteria. Biochemistry 40: 3232-3241

Zhang D, Mauzerall D (1996) Volume and enthalpy changes in the early steps of bacteriorhodopsin photocycle studied by time-resolved photoacoustics. Biophys J 71: 381-388

Zybailov B, van der Est A, Zech SG, Teutloff C, Johnson TW, Shen G, Bittl R, Stehlik D, Chitnis PR, Golbeck JH (2000) Recruitment of a foreign quinone into the A_1 site of photosystem I. II. Structural and functional characterization of phylloquinone biosynthetic pathway mutants by electron paramagnetic resonance and electron-nuclear double resonance spectroscopy. J Biol Chem 275: 8531-8539

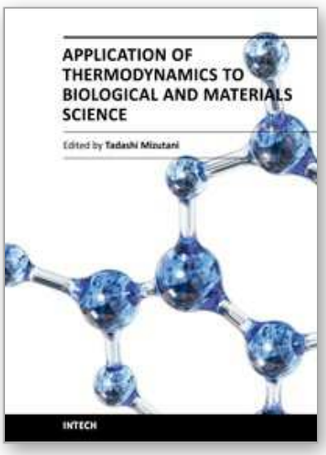

Application of Thermodynamics to Biological and Materials Science

Edited by Prof. Mizutani Tadashi

ISBN 978-953-307-980-6
Hard cover, 628 pages
Publisher InTech
Published online 14, January, 2011
Published in print edition January, 2011

Progress of thermodynamics has been stimulated by the findings of a variety of fields of science and technology. The principles of thermodynamics are so general that the application is widespread to such fields as solid state physics, chemistry, biology, astronomical science, materials science, and chemical engineering. The contents of this book should be of help to many scientists and engineers.

How to reference

In order to correctly reference this scholarly work, feel free to copy and paste the following:

Harvey J.M. Hou (2011). Enthalpy, Entropy, and Volume Changes of Electron Transfer Reactions in Photosynthetic Proteins, Application of Thermodynamics to Biological and Materials Science, Prof. Mizutani Tadashi (Ed.), ISBN: 978-953-307-980-6, InTech, Available from: http://www.intechopen.com/books/application-of-thermodynamics-to-biological-and-materials-science/enthalpy-entropy-and-volume-changes-of-electron-transfer-reactions-in-photosynthetic-proteins

INTECH
open science | open minds

InTech Europe
University Campus STeP Ri
Slavka Krautzeka 83/A
51000 Rijeka, Croatia
Phone: +385 (51) 770 447
Fax: +385 (51) 686 166
www.intechopen.com

InTech China
Unit 405, Office Block, Hotel Equatorial Shanghai
No.65, Yan An Road (West), Shanghai, 200040, China
中国上海市延安西路65号上海国际贵都大饭店办公楼405单元
Phone: +86-21-62489820
Fax: +86-21-62489821

IntechOpen